Annals of Phytomedicine 11(2): 378-384, 2022

DOI: http://dx.doi.org/10.54085/ap.2022.11.2.45

Annals of Phytomedicine: An International Journal

http://www.ukaazpublications.com/publications/index.php

Print ISSN : 2278-9839 Online ISSN : 2393-9885

Original Article : Open Access

Synthesis and *in vitro* antitubercular activity of some chroman derivatives

R.K. Kushwaha, Kuldeep Singh*,◆, D. Chandra** and P. Kumar***

**Faculty of Pharmacy, Integral University, Lucknow-226026, Uttar Pradesh, India*

*** G.C.R.G. College of Pharmacy, Lucknow-226201, Uttar Pradesh, India*

Article Info

Article history

Received 1 August 2022

Revised 16 September 2022

Accepted 17 September 2022

Published Online 30 December-2022

Keywords

Benzopyran

Antitubercular

Microplate alamar blue assay

Minimum inhibitory concentration

Docking

Abstract

Chromans are significant heterocyclic substances that can be created in a lab and are also naturally present in plants. They serve as a form of therapy such as antibreast cancer, antiestrogens, antitubercular and anticonvulsant, *etc*. The derivatives (ethyl 4-(substituted-2-hydroxyphenyl)-7-hydroxy-2-methyl-4H-chromene-3-carboxylate) were successfully synthesized using the intermediate ethylbenzylidine oxabutanoate. The proposed mechanism of the reaction is the Michael addition reaction. The resorcinol molecule functions as a nucleophile and the ethyl benzylidine oxabutanoate acts as a conjugated diene. These two compounds interact with one another to produce chroman derivatives. For the synthesis of benzopyran, this plan is highly efficient. Using autodock freeware software, designed compounds were studied for their antitubercular activity with target protein (InhA) enoyl-acyl carrier protein reductase (4fdo) receptor. According to a docking study, every compound has antitubercular activity. The drug isoniazid was used as standard in the biological studies for *in vitro* antitubercular activity on the MTB H37Rv strain. At the result of the assay, the pink color in the wells shows bacterial growth, whereas the blue color in the wells shows no bacterial growth. The minimum inhibitory concentration (MIC) was calculated. No MIC was seen in the *in vitro* antitubercular activity study up to the concentration of 64 µg/ml.

1. Introduction

One of the top 10 global causes of death is tuberculosis (TB). According to a 2021 WHO report, there were 10 million new cases of TB worldwide and 1.5 million people died from the disease (Global tuberculosis report, October 2021). Multidrug-resistant (MDR) TB cases were discovered in about 0.5 million new cases. Therefore, a new antitubercular drug with high efficacy and low toxicity is needed for a better TB cure (Khan *et al.*, 2017).

For the development of a new antitubercular drug, heteroatoms O, N, or S in heterocyclic compounds are useful. A good example of a heterocyclic compound that contains oxygen is benzopyran (chroman/chromene) nucleus. The chroman moiety is well known to possess a wide range of biological potentials, including those for contraception (Angelova *et al.*, 2017; Kumar and Gullaiya, 2014), analgesia, antibacterial, antifungal, antitubercular, anticancer, and anticonvulsant activity. Chromans were created (Friden *et al.*, 2012; Raj and Lee, 2020; Vekariya *et al.*, 2014; Simelane and Moshapo, 2020; Rawat and Verma, 2016; Demirayak and Yurttas, 2017) using a variety of methods, including tandem addition/cyclization of alkenyl aldehyde (Huang, 2020) and reduction of chromones (Volodimyr, 2010; Sethumathi *et al.*, 2021; Shailaja *et al.*, 2021; Thakur et al., 2020; Bouatrous, 2019).

Acid-catalyzed benzopyran formation through the Michael addition reaction shown in Figure 1 is one potential mechanism for scheme (Figure 2). The chroman derivatives were created in scheme by Michael addition of resorcinols with intermediate ethyl-benzylidine oxabutanoate while TFA was present. Using the base L-proline, the reaction was carried out by heating at 80°C the substituted aromatic aldehydes 1 and ethylacetoacetate 2 in DMSO. The variety of intermediate 3 is produced by the reaction. Under the most favourable reaction conditions, these intermediates 3 (ethylbenzylidine oxabutanoate) that have various substituents on the aromatic ring interact with resorcinol. Benzopyran derivative yields were satisfactory (Priyanka Sharma 2018; Rathod *et al.*, 2017; John A. Hyatt, 2007; Shitara *et al.*, 2000; Sharma and Chakraborty, 2019).

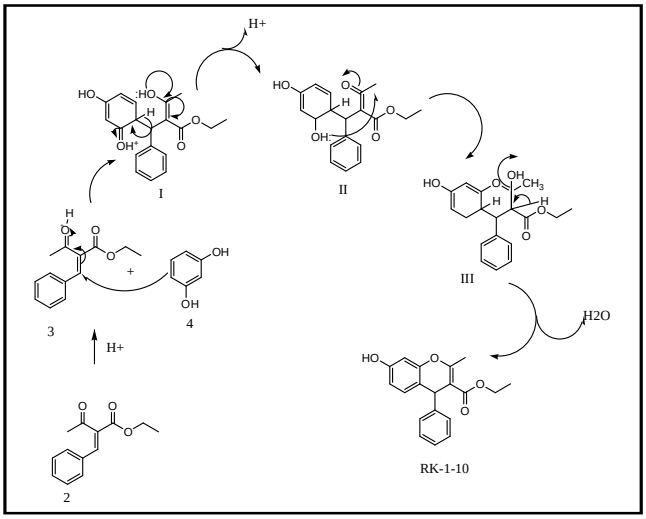

Figure 1: Michael addition reaction between resorcinol and ethylbenzylidin eoxabutanoate.

Corresponding author: Dr. Kuldeep Singh

Professor, Faculty of Pharmacy, Integral University, Lucknow-226026, Uttar Pradesh, India

E-mail: kuldeep@iul.ac.in

Tel.: +91-9453604762

2. Material and Methods

2.1 General procedure

All of the chemicals used in the synthesis of the compounds were analytical grade and bought commercially from Spectrochem and Avra Synthesis Pvt. Ltd. The 500 ml round bottom flask (RBF) was clean and previously dried. It was then charged with 1 mol of aromatic aldehyde (Figure 3), 1 mol of ethylacetoacetate and 30 mol % L-proline in DMSO. The mixture was then refluxed for 6 to 8 h at 80ºC. Following the successful completion of the reaction, additional research was conducted to enable the synthesis of the desired derivatives. In 500 ml of RBF, the 1.2 mmol of intermediate ethyl-benzylidine oxabutanoate (3) and 1 mmol of various resorcinols (4) were added. 5 ml of nitromethane and 1 mmol of TFA were added to this and refluxed for the next 4 to 7 h. The TLC profile in the methanol chloroform (1:99) mixture was used to monitor the reaction's progress. All synthetic compounds had their melting points (M.P.) measured using the open glass capillary method. The scheme shows the synthetic route leading to the test compounds RK-1 to RK-10 (Figure 7). The known method was used to create the chroman derivatives (Priyanka Sharma, 2018).

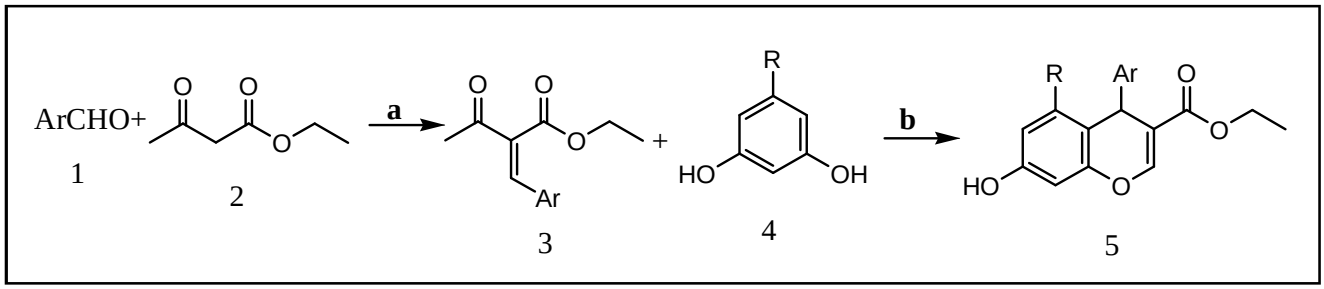

Figure 2: Scheme, synthetic pathway for final derivative RK-1 to RK-10. (a) L-proline (30 mol %), DMSO, 80°C, 8h, (b) TFA, CH_3NO_2, reflux, 4-7 h. (4) R= H or OH for different resorcinols.

ArCHO=

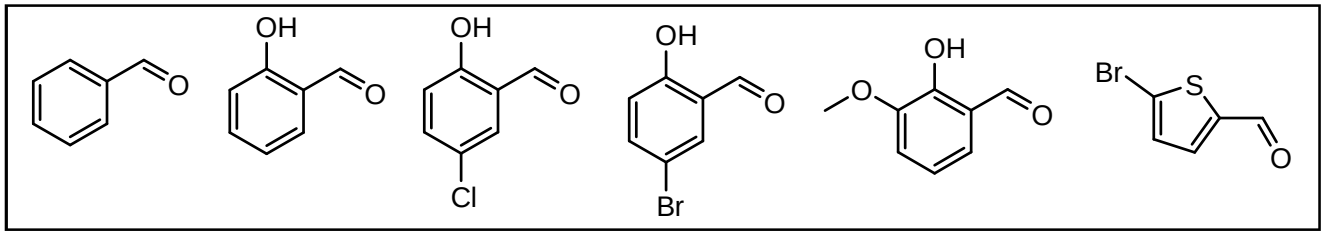

Figure 3: Aromatic aldehydes for obtaining variety of intermediate ethyl-benzylidine oxabutanoate.

2.2 Molecular docking

The understanding of target-receptor binding interaction is frequently used in the modern drug design context by means of molecular docking. The enoyl-ACP reductase (InhA) enzyme mainly function as in the synthesis of cell wall of MTB and for the purpose of identifying the ideal conformation, molecular docking experiments were conducted with the MTB enoyl-ACP reductase (InhA).

2.2.1 Target cleaning and preparation

The crystal structure of the target protein and the (InhA) enoyl-acyl carrier protein (Figure 4) reductase receptor obtained from the PDB (protein data bank; http://www.rcsb.org). For 3D protein structural data derived from various experimental studies, PDB is a widely used source. The protein under investigation has PDB ID 4fdo. For the analysis of the target proteins' surface-accessible pockets and interior-inaccessible cavities, the CASTp (computed atlas of surface topography of protein) server was used. After the target protein's 3D structure has been fully procured, use auto dock to add polar hydrogen, mark non-polar hydrogen bonds and add Kollman charge.

2.2.2 Legand cleaning and preparation

All of the suggested compounds, 2D structures were created in the program chemdraw and their 3D structures were downloaded from the website CORINA classic. PDB file preparation using the open babel version. The removal of structural strain and 3D structural correction were carried out with the aid of merck method of force field (MMFF), and then gasteiger charge and torsions were added using auto dock. The energy minimization and structure optimization of proposed compounds are very significant parameters. Isoniazid's crystal structure, a reference standard drug, was acquired from Pubchem.

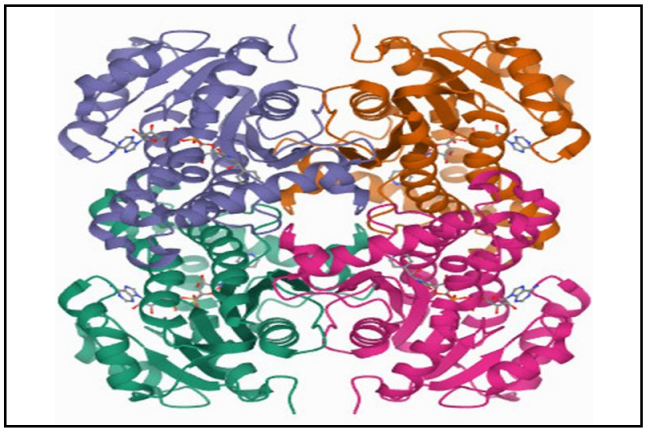

Figure 4: Enoyl-acyl carrier protein structure (InhA).

2.2.3 Molecular docking by auto dock vina

A computer program called auto dock vina is used to determine how a drug and a target protein will interact. It provides the least amount of interaction energy between the drug ligand and the target protein while exploring all of the system's degrees of freedom. It makes use of the empirical scoring function and the Lamarckian genetic algorithm and it provides reproducible docking results for drug ligands with about ten flexible bonds. Set the grid parameters and the x, y, and z centers for the docking analysis from auto dock vina (Rawat and Verma, 2021). Docking interaction energy is generated using auto dock vina of designed compounds (Figure 5 and Figure 6) shown in Table 2.

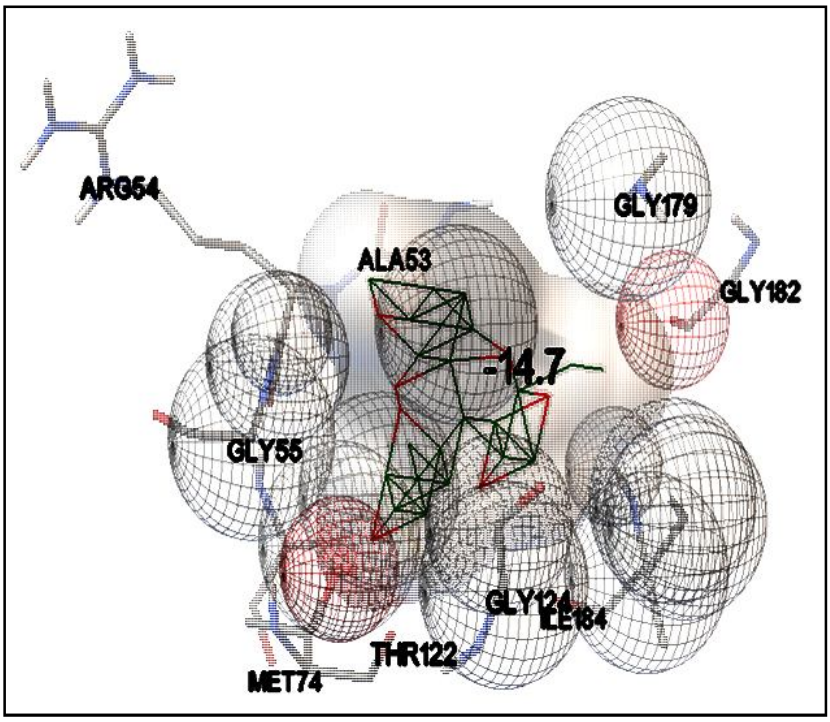

Figure 5: 3D structure of docking compound RK-7 with InhA (4fdo).

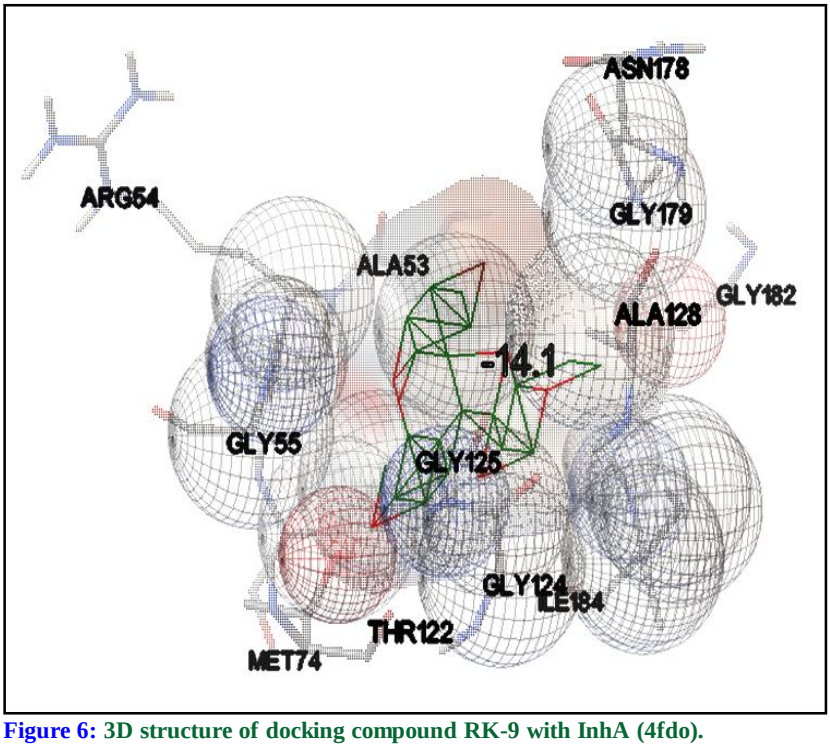

Figure 6: 3D structure of docking compound RK-9 with InhA (4fdo).

2.3 Biological activity

Agar dilution, broth dilution and broth microdilution are three methods used to test the ability of microorganisms to produce visible growth on a variety of agar plates, in broth-filled tubes and in microplate wells containing antimicrobial agent dilutions. The MIC is described as the lowest antibiotic concentration that stops bacteria from growing visibly. Stock solutions were prepared by using a formula. Plates were prepared with test and standard compound concentrations of 0.03, 0.06, 0.125, 0.25, 0.5, 1, 2, 4, 8, 16, 32 and 64 µg/ml. Before moving, the plates were kept aside to reach room temperature. Dried in a clean, laminar-flow cabinet. Each strain was incubated for 48 h at 36°C. Using an automatic micropipette, 5 µl of each bacterial suspension from each strain was added to the surface of the culture medium as an inoculum (usually 15-20 drops per plate). Until the drops were absorbed, plates were placed in a sterile laminar flow cabinet. Plates were incubated for 48 h at 36°C ± 1. It was confirmed that each tested strain had developed on the plate control without antibiotics after incubation. The pink colour was interpreted as bacterial growth, while the blue color indicated no bacterial growth. One or two colonies growing or a thin film of growth should not be taken seriously.

3. Results

By using 20 per cent ethyl acetate in hexane as the solvent, column chromatography was used to purify all compounds. The analysis of ^{1}H NMR, ^{13}C NMR, FT-IR, and melting points confirmed the final product. Table 1 presents physical and analytical information about synthesized derivatives.

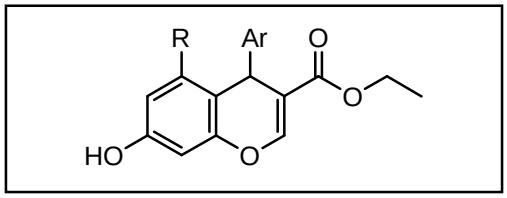

Figure 7: General structure of final compounds.

Table 1: Physicochemical and analytical data of synthesized compounds (Figure 7).

Compound	R	Ar	Reaction time (h)	Molecular formula	Mol. Weight	% yield	Melting point
RK-1	H		5	$C_{19}H_{18}O_5$	326.34	71	148-152
RK-2	H	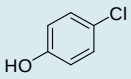	6	$C_{19}H_{17}ClO_5$	360.07	65	154-157
RK-3	H	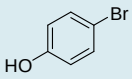	6.5	$C_{19}H_{17}BrO_5$	404.23	64	168-172
RK-4	H		6.5	$C_{17}H_{15}BrO_4S$	395.26	65	109-112
RK-5	H	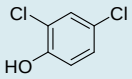	5	$C_{19}H_{16}O_5Cl_2$	395.23	76	101-104
RK-6	OH		4	$C_{19}H_{18}O_6$	342.34	80	149-153
RK-7	OH		5	$C_{20}H_{20}O_7$	372.36	73	118-121
RK-8	OH	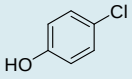	4.25	$C_{19}H_{17}ClO_6$	376.78	75	161-164
RK-9	OH	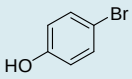	4	$C_{19}H_{17}BrO_6$	421.23	76	172-175
RK-10	OH		5	$C_{17}H_{15}BrO_5S$	411.26	75	129-132

3.1 NMR (^{1}H NMR and ^{13}C NMR) spectrum study

Ethyl 4-(2-hydroxyphenyl)-7-hydroxy-2-methyl-4H-chromene-3-carboxylate (RK-1) ^{1}HNMR (400MHz, $CDCl_3$, ppm)- δ1.12-1.16 (t, 3H, CH_3, *J*=8 Hz,), δ1.97 (s, 3H, CH_3), δ3.14 (s, 1H, OH), δ4.06-4.12 (m, 2H, >CH_2), δ4.20 (s, 1H, OH), δ6.32 (s, 1H, >CH), δ6.35 (s, 1H, >CH), δ6.83-6.87 (m, 2H, >CH), δ6.97-6.99 (d, 1H, *J*=8 Hz, >CH), δ7.05-7.09 (m, 1H, >CH), δ7.13-7.15 (d, 1H, *J*=8 Hz, >CH), IR (KBr, ν_{max}, cm^{-1}): 3385.20 (ν, -OH str), 2986.39 (ν, -CH str.), 2941.73 (ν, -CH str), 1719.78 (ν,C=O str), 1303.22 (ν, C-O str), 1506.3 (C=C str).

3.1.2 Ethyl-7-hydroxy-4-(5-chloro-2-hydroxyphenyl)-2-methyl-4H-chromene-3-carboxylate (RK-2) δ1.12-1.15 (t, 3H, CH_3, *J*=8 Hz), δ1.96 (s, 3H, CH_3), δ3.10 (s, H, OH), δ4.06-4.11 (m, 2H, >CH_2), δ4.26 (s, 1H, OH), δ6.34-6.37 (m, 2H, >CH), δ6.76-6.78 (m, 1H, >CH), δ6.97-6.99 (d, 1H, >CH, *J*=8 Hz), δ7.01-7.04 (d, 1H, >CH, *J*=8 Hz) δ7.12 (m, 1H, >CH), IR (KBr, ν_{max}, cm^{-1}): 3372.93 (ν, -OH str.), 3001.66 (ν, -CH str.), 2939.87 (ν, -CH str), 1717.88(C=O str), 1190.77(C-O str).

Ethyl-7-hydroxy-4-(5-bromo-2-hydroxyphenyl)-2-methyl-4H-chromene-3-carboxylate (RK-3) δ1.12-1.16 (t, 3H, CH_3, *J*=8 Hz), δ1.96 (s, 3H, CH_3), δ3.09-3.10 (s, 1H, OH), δ4.06-4.11 (m, 2H, >CH_2), δ4.16 (s, 1H, OH), δ6.36-6.37 (m, 2H, >CH), δ6.71-6.73 (d, 1H, >CH, *J*=8 Hz), δ6.96-6.99 (d, 1H, >CH, *J*=8 Hz), δ7.15-7.18 (d, 1H, >CH, *J*=8Hz) δ7.26-7.27 (m, 1H, >CH,).

Ethyl-7-hydroxy-4-(5-bromothiophen-2-yl)-2-methyl-4H-chromene-3-carboxylate (RK-4)^{1}HNMR (400MHz, $CDCl_3$, ppm)- δ1.26-1.29 (t, 3H, CH_3 *J*=8 Hz), δ2.43 (s, 3H, CH_3), δ4.16-4.23 (m, 2H, >CH_2), δ5.18 (s, 1H, OH), δ6.44 (d, 1H, thiophenyl-H, *J*=4 Hz), δ6.52 (s, 1H, >CH), δ6.56-6.58 (d, 1H, >CH, *J*=8 Hz), δ6.75 (d, 1H, thiophenyl-H, *J*=8 Hz), δ7.00-7.02 (d, 1H, >CH, *J*=8 Hz).^{13}C NMR (200 MHz, $CDCl_3$) - δ14.32, δ19.77, δ36.12, δ103.26, δ105.87, δ110.60, δ112.53, δ115.85, δ124.12, δ129.39, δ129.92, δ150.41, δ152.41, δ155.61, δ161.10, δ166.99.

Ethyl-5, 7-dihydroxy-4-(phenyl)-2-methyl-4H-chromene-3-carboxylate (RK-5) ^{1}HNMR (400MHz, $CDCl_3$, ppm)- δ1.21-1.24 (t, 3H, CH_3, *J*=8 Hz), δ2.10 (s, 1H, OH), δ2.43 (s, 3H, CH_3), δ4.07-4.13 (m, 2H, >CH_2), δ5.01 (s, 1H, OH), δ6.01 (s, 1H, >CH), δ6.17 (s, 1H, >CH), δ7.13-7.17 (m, 1H, >CH), δ7.22-7.24 (m, 2H, >CH), δ7.27-7.29 (m, 2H, >CH).

Ethyl-2-methyl, 4-(2-hydroxyphenyl), 5, 7-dihydroxy-4Hchromene-3-carboxylate (RK-6) ^{1}HNMR (400MHz, DMSO-d_6, ppm)- δ1.06-1.09 (t, 3H, CH_3, *J*=8 Hz), δ1.87 (s, 3H, CH_3), δ3.32 (s, 1H, OH), δ3.97-4.09 (m, 2H, >CH_2), δ4.50 (s, 1H, OH), δ5.67 (s, 1H, >CH), δ5.85 (s, 1H, >CH), δ6.77-6.79 (d, 1H, >CH, *J*=8 Hz), δ6.82-6.86 (t, 1H, >CH, *J*=8 Hz), δ7.04-7.08 (t, 1H, >CH, *J*=8 Hz), δ7.26-7.28 (d, 1H, >CH, *J*=8 Hz), δ9.09 (s, 1H, OH), δ9.50 (s, 1H, OH). ^{13}C NMR (200 MHz, DMSO-d_6) - δ14.33, δ25.99, δ30.16, δ61.11, δ94.47, δ96.34, δ98.11, δ103.10, δ115.93, δ121.43, δ127.55, δ127.82, δ128.24, δ151.46, δ152.92, δ155.48, δ157.16, δ169.20.

Ethyl-2-methyl, 4-(2-hydroxy-5-methoxyphenyl), 5, 7-dihydroxy-4Hchromene-3-carboxylate (RK-7) ^{1}HNMR (400MHz, DMSO-d_6, ppm)- δ1.05-1.09 (t, 3H, CH_3, *J*=8 Hz), δ1.87 (s, 3H, CH_3), δ3.32 (s, 1H, OH), δ3.71 (s, 3H, CH_3), δ3.96-4.08 (m, 2H, >CH_2), δ4.50 (s, 1H, >CH), δ5.67 (s, 1H, >CH), δ5.84 (s, 1H, >CH), δ6.77-6.80 (m, 2H, >CH), δ6.86-6.88 (d, 1H, >CH, *J*=8 Hz), δ9.08 (s, 1H, OH), δ9.47 (s, 1H, OH). ^{13}C NMR (200 MHz, DMSO-d_6) - δ14.32, δ25.99, δ30.09, δ43.60, δ55.95, δ61.10, δ94.41, δ96.31, δ97.98, δ103.08, δ110.96, δ119.37, δ121.32, δ128.49, δ140.53, δ147.56, δ153.04, δ155.44, δ157.15, δ169.22.

Ethyl-2-methyl, 4-(5-chloro-2-hydroxyphenyl), 5, 7-dihydroxy-4Hchromene-3-carboxylate (RK-8) ^{1}HNMR (400MHz, $CDCl_3$, ppm)- δ1.15-1.19 (t, 3H, CH_3, *J*=8 Hz), δ1.93 (s, 3H, CH_3), δ2.59 (s, 1H, OH), δ3.06 (s, 1H, OH), δ4.08-4.12 (m, 2H, >CH_2), δ4.57 (s, 1H, >CH), δ5.85 (s, 1H, >CH), δ5.95 (s, 1H, >CH), δ5.73-5.75 (d, 1H, >CH, *J*=8 Hz), δ6.99-7.01 (d, 1H, >CH, *J*=8 Hz), δ7.31 (s, 1H, OH).

Ethyl-2-methyl, 4-(5-bromo-2-hydroxyphenyl), 5, 7-dihydroxy-4Hchromene-3-carboxylate (RK-9) ^{1}HNMR (400MHz, $CDCl_3$, ppm)- δ1.15-1.19 (t, 3H, CH_3, *J*=8 Hz), δ1.93 (s, 3H, CH_3), δ3.05-(s, 1H, OH), δ4.09-4.14 (m, 2H, >CH_2), δ4.58 (s, 1H, OH), δ5.83 (s, 1H, >CH), 5.96 (s, 1H, >CH), δ6.69-6.71 (d, 1H, >CH, *J*=8 Hz), δ7.13-7.16 (d, 1H, >CH, *J*=4 Hz), δ7.46 (d, 1H, >CH).

Ethyl-2-methyl, 4-(5-bromothiophene-2-yl), 5, 7-dihydroxy-4Hchromene-3-carboxylate (RK-10) ^{1}HNMR (400MHz, $CDCl_3$, ppm)- δ1.28-1.32 (t, 3H, CH_3, *J*=8 Hz), δ2.41 (s, 3H, CH_3), δ4.20-4.24 (m, 2H, >CH_2), δ5.32 (s, 1H, OH), δ6.09-6.10 (d, 1H, >CH, *J*=4 Hz), δ6.15-6.16 (d, 1H, >CH, *J*=4 Hz), δ6.54-6.55 (d, 1H, >CH, *J*=4 Hz), δ6.76-6.77 (d, 1H, >CH, *J*=4 Hz), ^{13}C NMR (200 MHz, $CDCl_3$) - δ14.37, δ19.72, δ31.34, δ60.75, δ96.18, δ99.55, δ104.45, δ106.17, δ110.70, δ124.72, δ129.26, δ150.83, δ151.55, δ153.94, δ156.01, δ161.22, 166.92.

3.2 Docking results

Target protein evaluations for molecular docking were conducted. It is renowned for their inhibiting effects. This study proposed chroman derivatives to the target receptors and docking tools (4fdo), keeping in mind the aforementioned structure. Utilizing binding affinity kcal/mol), the interaction profile was assessed. In the auto dock vina docking tool, all the compounds exhibit good binding affinities between – 12.9kcal/mol and – 4.7 kcal/mol (Table 2). Since the interaction between the most valuable proposed compounds and Isoniazid (–6.5 kcal/mol) was higher, this is what was discovered.

3.3 Biological activity

The microplate alamar blue Assay (MABA) method was used to assess the biological activity of the synthetic compounds in the series (RK-1 to RK-10) against the *Mycobacterium tuberculosis* MTB H37Rv strain (Lima and Henrques, 2011; Shetye *et al.*, 2021). Isoniazid was the drug of choice. At the conclusion of the experiment, the blue wells showed no bacterial growth while the pink wells displayed bacterial growth. The Table 2 below displays the interaction energy and MIC values that were as a result.

Table-2: Docking interaction energy (using auto dock vina) and MICs of test compounds (RK-1 to RK-10).

S. No.	Code	4fdo binding affinity kcal/mol	MIC(µg/ml) *M. tuberculosis* H37Rv ATCC 27294
1.	RK-1	-13.9	>64
2.	RK-2	-14.0	>64
3.	RK-3	-13.8	>64
4.	RK-4	-13.3	>64
5.	RK-5	-13.8	>64
6.	RK-6	-14.0	>64
7.	RK-7	-14.7	>64
8.	RK-8	-14.0	>64
9.	RK-9	-14.1	>64
10.	RK-10	-12.9	>64
11.	Isoniazid	-6.5	0.03

4. Discussion

Chromans and their derivatives are widely used and have a variety of medicinal uses. Current research demonstrates that substituted chromans are clearly essential for the good anti-TB activity. A number of studies claim that chromans is used as an efficient antitubercular agent. We discussed a quick and secure method for creating ethyl 4-(substituted-2-hydroxyphenyl)-7-hydroxy-2-methyl-4H-chromene-3-carboxylate with chroman nuclei (Figure 2: Scheme). Using ethylbenzylidine oxabutanoate (3) and resorcinols shown in Figure 3 in the presence of trifluoro acetic acid and nitromethane yielded (64-80% yields) compound RK-1 to RK-10. Physical data of compounds included in the Table 1.

The docking studies of each designed compound were performed by using the freeware software auto dock vina. The 3D structure of the target protein receptor (InhA) was obtained from PDB and has PDB ID 4fdo. All the designed compounds exhibited good binding affinities between 12.9 kcal/mol and 14.7 kcal/mol. This indicates that all the designed compounds have good antitubercular activity.

On the JEOL ECX-400 spectrometer, NMR spectra were recorded at 400 MHz for ^{1}H and 200 MHz ^{13}C NMR in DMSO-d_6 and $CDCl_3$. Chemical shifts (δ) in relation to TMS were calculated in parts per million (ppm). On a Perkin Elmer Spectrum Version 10.03.06 spectrophotometer, the FTIR spectra (KBr) of the samples were examined. The formation of RK-1 to RK-10 was revealed by the NMR spectra of derivatives.

The MABA method was used to calculate the MIC values. The assay was carried out in a 96-well microplate. The test and standard compound dilutions ranged in concentration from 0.03 µg/ml to 64 µg/ml. At the conclusion of the experiment, it was discovered that the synthetic compounds did not prevent bacterial growth up to a concentration of 64 µg/ml.

5. Conclusion

Successful synthesis of the chroman derivatives was accomplished and evaluated for their antitubercular activity. The current study reports that the series of chroman derivatives RK-1 to RK-10 do not exhibit antitubercular activity because in the *in vitro* antitubercular activity study, no MIC was detected up to a concentration of 64 µg/ml. Additional molecular docking research suggests that all the compounds exhibit good binding affinities between –12.9 kcal/mol and – 14.7 kcal/mol. Therefore, these substances may be used as lead substances for future research.

Acknowledgements

Integral University and G.C.R.G. College of Pharmacy provided a research facility, which the authors are grateful for. We appreciate C.D.R.I. Lucknow's assistance with the biological study and spectral facility. Manuscript number provided by the Research and Development Committee is IU/R & D/2022-MCN0001666.

Conflict of interest

The authors declare no conflicts of interest relevant to this article.

References

Angelova, V.; Valcheva, V. and Pencheva, T. (2017). Synthesis, antimycobacterial activity and docking study of 2-aroyl-(1) benzopyrano (4,3-c)pyrazol-4(1H)-one derivatives and related hydrazide-hydrazones, Bioorganic and Medicinal Chemistry Letters, **27**(13):2996-3002.

Bouatrous, Y. (2019). Antibacterial activity of an essential oil and various extracts of the medicinal plant *Thymus hirtus* sp. *algeriensis* Boiss. and Reut. Ann. Phytomed., **8**(2):100-105

Demirayak, S. and Yurttas, L. (2017). New chroman-4-one/thiochroman-4-one derivatives as potential anticancer agents. Saudi Pharmaceutical Journal, **25**(7):1063-1072.

Friden-Saxin, M; Seifert, T. and Landergren, M. (2012). Synthesis and evaluation of substituted chroman-4-one and chromone derivatives as sirtuin 2-selective inhibitors, Journal of Medicinal Chemistry, **55**(16):7104-7113, .

Huang, H. L. (2020). Visible-light-promoted cascade radical cyclization: Synthesis of chroman-4-ones and dihydroquinolin-4-ones. The Journal of Organic Chemistry, **85**:3963-3972.

John, A. Hyatt (2007). Convenient preparation of 2, 7, 8 trimethyl 6 hydroxychroman 2 carboxylic acid (γ Trolox), Synth. Commun., **38**(1):8-14.

Kakkar (2018). Design, synthesis and biological evaluation of 3 (2 aminooxazol 5 yl) 2H chromen 2 one derivatives Chemistry Central Journal, **12**:130.

Kumar, A. and Gullaiya, S. (2014). Contraceptive activity of 4-(4-hydroxy-3-methyl-hex-5-enyl)-chroman-2,7-diol *via* inhibiting ovulation in gonadotropin-primed immature rat model, Biomedicine and Aging Pathology, **4**(1):43-47.

Khan, Y. S.; Osman, H. and Khan, M. S. (2017). Design, characterization *in vitro* antibacterial, antitubercular evaluation and structure activity relationships of new hydrazinyl thiazoilyl coumarin derivatives, Med. Chem. Res., **26**(6):1139-1148.

Lima, C. H. S. and Henriques, G. M. O. (2011). Synthesis and antimycobacterial evaluation of N-(E)-heteroaromaticpyrazine-2-carbohydrazide derivatives. Medicinal Chemistry, **7**(3):245-249.

Priyanka Sharma, R. K. (2018). Facile construction of 4H-chromenes *via* Michael addition of phenols to benzylidene oxobutanoates and their successful conversion into pyranocoumarins. Tetrahedron Lett., **59**(24):2347-351.

Rawat, P. and Verma, S. M. (2016). Design and synthesis of chroman derivatives with dual anti-breast cancer and antiepileptic activities. Dove Press Journal. **14**:139.

Rathod, A.; Godipurge, S. and Biradar (2017). Synthesis of indole, coumarinyl and pyridinyl derivatives of isoniazid as potent antitubercular and antimicrobial agents and their molecular docking studies, International Journal of Pharmacy and Pharmaceutical Sciences, **9**(12):233.

Raj, V. and Lee, J. (2020). 2H/4H-Chromenes-A Versatile Biologically Attractive Scaffold, Front. Chem, 8:623.

Rawat, P. and Verma, S. M. (2021). Docking studies and evaluation of antimicrobial activity of chroman carboxamide derivatives, Indian Journal of Pharmaceutical education and Research, **55**(1):S275-S284.

Shetye, G. S., Choi, K. B., Kim, C. Y., Franzblau, S. G. and Cho, S. (2021). In vitro profiling of antitubercular compounds by rapid, efficient, and nondestructive assays using autoluminescent mycobacterium tuberculosis. Antimicrobial Agents and Chemotherapy, **65**(8):230.

Sharma, S. and Chakraborty, D. (2019). Original article Antimicrobial and antioxidant activity of Coriandrum sativum L., Ann. Phytomed., **8**(1):135-139.

Shitara, H.; Aoki, Y.; Hirose T. and Nohira H., (2000). Synthesis of optically active 2-methylchroman derivatives and application to chiral dopants for nematic liquid crystals. Bull. Chem. Soc. Jap., **73**:259-265.

Sethumathi, P. P.; Manjuparkavi, K.; Lalitha, V.; Sivakumar T.; Menaka, M.; Jayanthi A. and Ashok Kumar, B. (2021). Evaluation of *in vitro* antioxidant and antimicrobial activity of polyherbal formulation of Thirikadugu chooranam and Parangipattai chooranam, Ann. Phytomed., **10**(2): 169-174.

Shailaja, P. Desai; Yasmin, H. Momin; Sneha, T. Taralekar; Yuvraj, D. Dange; Sneha, R. Jagtap and Harshad, P. Khade (2021). Evaluation of potential *in vitro* anticancer and antimicrobial activities of synthesized 5-mercapto-4-substituted 1, 2, 4 triazole derivatives, Ann. Phytomed., **10**(2): 273-279

Simelane, S. and Moshapo, P. (2020). Benzopyran-Core as an Antimycobacterial Agent,Organic and Medicinal Chemistry International Journal, **10**(2):133-154.

Thakur, K.; Mini Mol, P.; Gawhankar, M.; Gupta, H, Patil, P.; Salmani, S. and Thakur, M. (2020). Physicochemical characterization and antimicrobial properties of Mahamanjishthadi kadha: An Ayurvedic formulation, Ann. Phytomed., **9**(1):78-90.

Vekariya, P.; Pandya, J. and Joshi, H. (2014). An efficient and facile synthesis of 1,2,4-Aryl triazoles and 4-thiazolidinones bearing 6-Fluorochroman Nucleus, Hindawi, pp:1-7.

Volodimyr, S. (2010). Synthesis of chroman-4-ones by reduction of chromones. Current Organic Syntheisis, **7**(3):239-253.

Citation **R.K. Kushwaha, Kuldeep Singh, D. Chandra and P. Kumar (2022). Synthesis and *in vitro* antitubercular activity of some chroman derivatives. Ann. Phytomed., 11(2):378-384. http://dx.doi.org/10.54085/ap.2022.11.2.45.**